Applied Energy 146 (2015) 122–134

Contents lists available at ScienceDirect

Applied Energy

journal homepage: www.elsevier.com/locate/apenergy

Development of a three-phase battery energy storage scheduling and operation system for low voltage distribution networks

Christopher J. Bennett, Rodney A. Stewart *, Jun Wei Lu

Griffith School of Engineering, Griffith University, Gold Coast Campus 4222, Australia

HIGHLIGHTS

- Forecast based 3-phase energy storage scheduling system for the LV network.
- Reduces peak demand through peak shaving and valley filling.
- Better manages distributed supply from solar PV through optimal battery charging.
- Load balances through intelligent charging and discharging.
- Developed system was tested using actual LV distribution network transformer data.

ARTICLE INFO

Article history:
Received 6 October 2014
Received in revised form 13 January 2015
Accepted 3 February 2015

Keywords:
Battery energy storage
Schedule
Forecast
Real time operator
Peak demand
Load balancing

ABSTRACT

Three phase battery energy storage (BES) installed in the residential low voltage (LV) distribution network can provide functions such as peak shaving and valley filling (i.e. charge when demand is low and discharge when demand is high), load balancing (i.e. charge more from phases with lower loads and discharge more to phases with higher loads) and management of distributed renewable energy generation (i.e. charge when rooftop solar photovoltaics are generating). To accrue and enable these functions an intelligent scheduling system was developed. The scheduling system can reliably schedule the charge and discharge cycles and operate the BES in real time. The scheduling system is composed of three integrated modules: (1) a load forecast system to generate next-day load profile forecasts; (2) a scheduler to derive an initial charge and discharge schedule based on load profile forecasts; and (3) an online control algorithm to mitigate forecast error through continuous schedule adjustments. The scheduling system was applied to an LV distribution network servicing 128 residential customers located in an urban region of South East Queensland, Australia.

1. Introduction

There has been a substantial push by governments to promote the installation of residential solar photovoltaic (PV) array installations in the low voltage (LV) distribution network through subsidies and feed-in-tariffs. In Australia, residential solar PV installations have been promoted by the Renewable Energy Target and the feed-in tariff schemes [1]. As of the 2012–13 financial year, the Australian Energy Regulator [1] reports that Australia's combined rooftop solar PV capacity is 2300 megawatts (MW). In South East Queensland (SEQ) the distribution network operator, Energex, noted that the number of customers with solar PV increased from 2000 to 221,000 installations from 2009 to June 2013, with 74,000 installations taking place between June 2012 and June 2013 [2]. The increase of customers with solar PV installations contributed to an increase price of energy, which led to a slight reduction in energy consumption from conventional sources and a shift in the SEQ network peak to later in the day [2,3].

Daily peak demand in residential networks typically occurs in the evenings in summer and both late morning and evening in winter [4]. Solar PV generation is dependent on the inclination of incoming solar radiation; hence, peak generation occurs during the middle of the day, typically when demand in the residential distribution network is low. Due to the behaviour of residential customers (i.e. concentrated energy demand activities in the evening) and the nature of solar PV generation, there is an incongruity between when energy is generated and when it is required. This can lead to power quality issues in the LV distribution network, such as overvoltage at points of common coupling and instances of reverse power flow to the distribution feeders [5]. In some

* Corresponding author. Tel.: +61 7 5552 8778.
E-mail addresses: christopher.bennett2@griffithuni.edu.au (C.J. Bennett), r.stewart@griffith.edu.au (R.A. Stewart), j.lu@griffith.edu.au (J.W. Lu).

http://dx.doi.org/10.1016/j.apenergy.2015.02.012
0306-2619/

Nomenclature

adj	loop adjustment constant
BE	battery bank efficiency (%)
C	capacity (kW h)
CT	charge target (W)
CR	charge rating (W)
e_a	energy available (kW h)
e_r	energy required (kW h)
edp	end of discharge period
EP	evening peak
DoD	depth of discharge (kW h)
DR	discharge rating (W)
DT	discharge target vector (W)
fe	finish element number
i	inverter or phase
iCR	inverter charge rating (W)
iDR	inverter discharge rating (W)
IE	inverter efficiency (%)
L	historical load (W)
Lf	load forecast (W)
LP	load profile (W)
LPf	forecasted load profile
m	gradient (W/t)
m_r	actual rate of energy use (W/t)
m_s	scheduler's rate of energy use (W/t)
min_r	estimated end of discharge period
min_s	scheduler's end of discharge period
MP	morning peak
np	next peak
pp	previous peak
se	start element number
SoC	state of charge (kW h)
SoC_s	scheduler's state of charge (kW h)
t	time iteration
t_α	amplitude threshold
TC	total charge (kW h)
t_m	gradient threshold (W/t)
α	amplitude (W)
δ_t	charge in charge (kW h)
ω	number of time intervals

circumstances remedial measures such as tap changes or more costly network augmentations are required to manage the excess of power produced. Since solar PV generation rarely coincides with peak demand periods in the residential LV network, solar PV fails to contribute to supporting the network through reducing peak demand [6].

The installation of distribution energy storage (DES) may be cost-effective in LV distribution networks with high penetrations of solar PV, load during peak demand period nearing the ratings limits of the LV transformer or unbalanced loads. The general concept is that the DES will charge from the grid during low demand periods or when solar PV is generating surplus energy and discharge during peak demand periods—known as 'peak shaving and valley filling' [7]. This concept will serve to level the demand profile, reduce peak demand and mitigate overvoltage and reverse power flow issues induced by high solar PV penetrations. A proven consistent reduction in peak demand derives value for the utility through electricity network augmentation capital expenditure deferrals. While historically DES has been viewed as a cost prohibitive for application in the LV network, advances in battery technology, feed-in-tariff schemes and the economy of scale effect from electrical vehicles, energy storage will become less cost prohibited in the future [7–9].

To be effective, DES scheduling systems must optimally charge during periods of high solar PV generation or low demand and discharge during periods of peak demand. Many methods have been proposed in the literature to achieve this objective. The most common methods include the use of optimisation algorithms to minimise or maximise objective functions or through finding the optimal solution through dynamic programming [10–23]. These systems achieve optimal solutions but their implementations are relatively complex. Alternatively, a less complex heuristics-based DES scheduling system that has been purpose-built to cater for the characteristics of the LV network and battery energy storage (BES), as proposed herein. The proposed scheduling system comprises three core components: (1) an expert system to forecast next day load profiles (Section 4.3); (2) a scheduling algorithm that interprets the forecasts and provides a charge and discharge schedule (Section 4.4); and (3) an online control algorithm to adjust the charging and discharging in real time to mitigate scheduling error (Section 4.5).

The remainder of this paper is structured in an additional five sections. Section 2 contains the literature review which highlights methods of DES scheduling and formulates the method of this research. The nature of the data used in this research is described in Section 3. A detailed method for developing the scheduling system and constituent components is presented in Section 4. Section 5 presents the initial schedule results from the scheduler, the online control system's actions to mitigate scheduling error and the results for a 72 h simulation of the scheduling system as a whole. The paper concludes in Section 6.

2. Literature

2.1. Energy storage scheduling systems

The literature has proposed a number of different methods to construct DES scheduling systems to achieve one or more objectives such as engaging in valley fill and peak shaving operations, mitigating power quality issues and utilising distributed renewable energy generators, such as solar PV and wind turbines [5,10,24,11–16,25,17–23]. For scheduling systems to calculate a schedule for BES, they must rely on information that allows for charging and discharging periods to be identified or inferred. Types of information that are relied on may include historical load data, load forecasts, time-of-use tariffs, energy market prices and costs of production. Methods used to calculate schedules include time-based heuristics, voltage or frequency set points, fuzzy logic controllers, objective function optimisation and dynamic programming [5,10,24,11–16,25,17–23].

2.2. Price signal based systems

Marwali et al. [11], Lu and Shahidehpour [12] and Koutsopoulos et al. [17] developed scheduling systems that aimed to minimise the production cost of supplying electricity while attempting to peak shave and valley fill. The scheduling systems developed by Marwali et al. [11] and Lu and Shahidehpour [12] involve the coordination of thermal generators and co-located solar PV and BES. Marwali et al. [11] separate the scheduling problem into three steps. The first step involves anticipating solar PV generation,

thermal commitment and by how much the BES is required to be charged. The second step uses Lagrangian relaxation to minimise thermal commitment cost based on the thermal objective function. The final step minimises the total cost objective function. Lu and Shahidehpour [12] follow similar steps as Marwali et al. [11] to solve an initial schedule. From there, an hour ahead optimal schedule is calculated via network flow programming and linear programming. Koutsopoulos et al. [17] assigns a convex cost function for instantaneous demand, which represents the increase cost as load increases. Demand in the network is treated as a Poisson process of power requests. A BES cost objective function is solved through a process of dynamic programming.

Scheduling systems developed by Sanseverino et al. [24], Hu et al. [16] and Grillo et al. [18] rely on price signals through the use of time-of-use tariffs, day-ahead energy market data, hour ahead market data and spot prices to optimise the charging and discharging of BES. The use of the day-ahead, hour-ahead and spot price markets gives the scheduling systems an accurate representation of what the load is going to be in the grid. A high price anticipates a high demand and a low price anticipates a low demand. The general principle behind these systems is to maximise profit or minimise cost of the operation of the BES. In turn, this is done through purchasing energy when the price is low (charging) and selling energy when the price is high (discharging). Sanseverino et al. [24] solves the schedule by a fuzzy logic controller. The controller is tuned based on past demand history and an economic indicator. The Hu et al. [16] and Grillo et al. [18] scheduling systems set up a cost or profit objective function that reflects the capital and operations costs of the BES and takes into account the energy price market. Hu et al. [16] solve the objective function through Lagrangian optimisation and Grillo et al. [18] solve the objective function through dynamic programming.

Lee [13] and Oudalov et al. [14] sought to reduce the energy supply cost of industrial customers. Industrial customers are charged for energy supplied by both time-of-use tariffs and the maximum demand they consume. Lee [13] and Oudalov et al. [14] proposed that through BES and adequate scheduling, their load can be reduced and they will receive lower energy costs. Lee [13] created an objective function representing the cost of energy to the industrial customer over a monthly period, which included the BES, and then used particle swarm optimisation to calculate the charge and discharge schedule. Oudalov et al. [14] outlined two dynamic programming based systems where the first sizes the BES and the second schedules. The sizing of the BES is based on historical load data to achieve maximum benefit, which is defined as savings in electricity minus the capital, maintenance and operational costs. Scheduling relies on the customers' load profile, energy supply costs, BES parameters and the target value of maximum load.

2.3. Forecast based systems

Matallanas et al. [19], Rowe et al. [21] and Rowe et al. [22] primarily rely on forecasting load to schedule the charging and discharging of BES. Matallanas et al. [19] designed an active demand side management (ADSM) system for a smart, energy efficient home with appliances, solar PV arrays and BES connected to a centralised controller. The user selects deferrable appliances, such as washing machines, to be used during the day. Load and solar PV forecasts are supplied to the central controller. The controller then uses a neural network (NN) to schedule deferrable appliances and the charging and discharging of BES so that the least load is exerted on the LV network. Castillo-Cagigal et al. [20] integrated the ADSM system developed by Matallanas et al. [19] with a BES control system for a residential premise with rooftop solar PV and BES. The goal of the BES control system is maximise the consumption of energy produced by the solar PV. The ADSM ensures that deferrable loads are scheduled for when solar PV is generating. Energy produced by the solar PV not consumed by the deferrable loads is allocated to charging the battery bank. Energy is supplied by the battery bank when solar PV generation is insufficient.

Rowe et al. [21] used a LV distribution network (household-level) forecasting technique developed by Haben et al. [26] to provide load profile forecasts. The demand profile forecast undergoes a filter stage whereby peak demand is altered in magnitude and period. The scheduler receives the altered forecast and iteratively calculates a discharge set point where above the set point the system is set to discharge and below the system is able to charge. Rowe et al. [22] further developed the scheduling system to include an online optimisation algorithm that operates by forecasting demand using a load scenario tree and optimises the schedule to maximise peak demand reduction.

2.4. Combined use of price signals and forecasts

Systems that use combined load and price forecasts provide advantages over pure price signal determined scheduling algorithms due to the ability for optimisation to take into account reducing peak demand and maximising value out of the systems. Jayasekara et al. [10] set out to schedule customer side co-located solar PV and BES to achieve peak shaving and valley fill objectives. The systems operates by first forecasting load a day ahead and then filtering the forecast using a Fourier series to provide a 24-h load profile forecast. Under the load profile forecast, the system minimises a daily operational cost objective function based on total battery cost, time-of-use tariffs and ratio of negative to positive sequence voltages. The system optimises the real time operation by use of the energy spot price. Xu et al. [15] developed an initial schedule based on the day ahead energy market through minimisation of a cost of energy objective function. Real time control is conducted through forecasting price and loads and the scheduling is balanced through a receding horizon control strategy. Similar to Jayasekara et al. [10], Riffonneau et al. [25] formulated a scheduling system that applies to co-located solar PV and BES. The system initialises by forecasting irradiance, temperature, load profile and the price of energy. The optimisation of the system seeks to achieve optimal peak reduction at least cost through dynamic programming.

The scheduling system developed by Arghandeh et al. [23] aimed at producing a charge discharge schedule through optimising an objective function through a gradient based heuristic approach. The objective function includes the cost of purchasing energy when charging, saving costs when discharging, load profile forecasts, local marginal price forecasts, feeder losses and energy storage system constraints. For each time interval the local marginal price is forecast, the load is forecast and the optimisation routine is run again to adjust the schedule before dispatch.

2.5. Set point and voltage control

The integration of residential rooftop solar PV causes power quality issues, such as voltage rise in some areas. Alam et al. [5] set out to use BES to mitigate power quality issues. The scheduling system responds in real time to voltage occurring at the point of common coupling. If the voltage is high (close to or above operational targets), the system sets the BES to charge. During the peak demand periods, voltage sag can occur. In response to voltage sag, the system sets the BES to discharge. In effect, the system follows the load occurring in the network to achieve elements of peak shaving and valley filling. Kabir et al. [27] proposed a central control system which dictates the injection into the grid of real and reactive power for customer located distributed solar PV and energy storage. Kabir et al. [27] first estimates the solar PV generation

using a discrete time Markov chain process. If the probability of solar PV generation is greater than 50% and the resistance/reactance ratio is greater than a critical threshold the energy storage systems are set to charge such to prevent overvoltage. To prevent voltage sag, the energy storage systems are set to discharge. Results displayed that the control system was able to keep the voltage on the network within statutory limits.

2.6. Problem formulation

Using one or more types of information about the electricity network and the BES, the scheduling systems in the literature predominantly employ optimisation routines or genetic programming [10–16,25,17–23]. Optimisation algorithms depend on the creation of an objective function composed of functions that represent the system which is to be scheduled [10–13,15,16,21–23]. These functions are in terms of costs or benefits for particular operations or components of the system. The optimisation of the objective function seeks to find a schedule that minimises a cost or maximises a benefit. Dynamic programming involves breaking the scheduling problem into a series of sub-problems, examines a range of scheduling solutions and chooses the highest performing [11,14,17,18]. The literature has conveyed that optimisation algorithms, dynamic programming and other methods of calculating a schedule work well for finding the optimal solution given system constraints and objective functions.

These techniques are relatively complex to implement and depend on formulating objective functions and constituent functions that accurately represent how the scheduling system should operate given certain states. Unless direct relationships can be identified, such as economic costs or benefits based on the operation of the BES and time-of-use tariffs or energy markets prices, formulating and weighting functions is reliant on trial and error.

To avoid complexity and with knowledge of how a scheduling system should operate and what an optimal schedule should achieve, there is an avenue of calculating schedules based on a heuristics approach. Thus, a heuristics approach could be a viable alternative to approaches involving more complex optimisation algorithms. Many regions, including SEQ, do not have energy storage tariff arrangements or localised network pricing. In the absence of price signal based information, the proposed heuristics approach for BES scheduling will depend on load forecasts. Similar to Xu et al. [15] and Arghandeh et al. [23], the proposed scheduling system will have a component which provides an initial schedule based on forecasts and an online component which adjusts the schedule in real time.

3. Data

Data used in this research was sourced from a residential LV distribution network transformer that was supplied by Energex (the distribution network operator for SEQ). The distribution transformer supplied 128 residential customers located in an inner suburb of Brisbane, Queensland. The provided dataset contains current, voltage and phase angle recordings at 10-min intervals and covers the period between the middle of January 2012 and the middle of February 2013. The phases of the network serviced by the transformer are unbalanced. Load experienced on one phase may not be indicative of load experienced on the other two phases. Weather data used were sourced from the Brisbane City weather station and made publically available by the Australian Bureau of Meteorology.

There are two distinct types of load profiles that occur in the network serviced by the transformer: the summer profile and the winter profile (see Fig. 1). The summer load profile is characterised

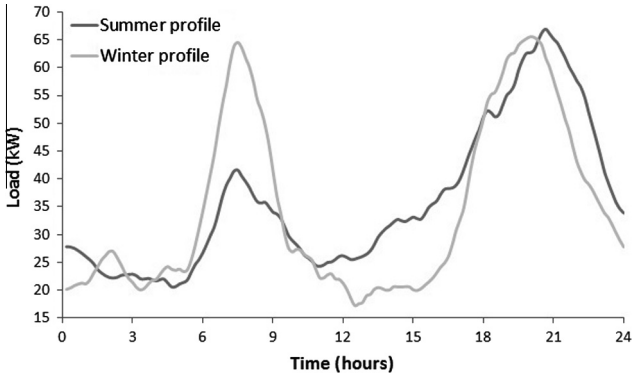

Fig. 1. Summer and winter load profiles.

by low load in the early morning, an increased load between 7 am and 10 am and a peak demand period, which occurs in the evening between 6 pm and 10 pm. The winter profile has low load during the early morning, a morning peak (MP) demand period between 6 am and 9 am, low demand during the middle of the day and an evening peak (EP) demand period between 6 pm and 10 pm. The magnitudes of the load in the MP demand period and EP demand period often differ. Days when load is high generally denote that the load during the EP demand period will be greater than the load during the morning period. Different permutations of the two distinct load profiles occur through the year based on external influences such as temperature, humidity, day of the week and exogenous events [4,28].

The fluctuations in load throughout the year are predominately a product of customers' uses of heating and cooling appliances in response to changes in temperature. Bennett et al. [28] observed that the load response to temperature is parabolic in nature and is able to account for half of the observed load. The relationship reflects consumers' propensities to utilise heating and cooling appliances in the warmer and cooler periods. Fig. 2 displays the magnitudes of the MP demand period and EP demand period throughout the year for phase 3. The MP remains relatively flat during periods of the year where temperature is average or warmer. The MP increases during colder periods of the year such as late autumn, winter and early spring. The EP demand is greatest during summer and winter and is relatively flat during autumn and spring.

4. Method

4.1. Overview

The operation of the proposed three-phase BES scheduling system for the LV distribution network is based on load forecasts. The system is designed to discharge during peak demand periods and charge the BES during periods when load is low and solar PV is generating. The BES is desired to be installed by the network operator and independent of co-located solar PV. Load forecasts provide the system information about the future to allow a schedule to be established. The LV distribution network typically has unbalanced phases; the load exhibits a high degree of variability and occurrences of random shocks [4,21,22,26,28]. The conditions of the LV distribution network, combined with high penetrations of solar PV on the network, lead to hampered load forecast accuracy in comparison to sections of the electricity network that supply a greater number of customers. In turn, there are two conditions that the scheduling system is required to operate under: (1) variable and unbalanced load conditions synonymous with LV distribution networks; and (2) imperfect load forecasts (i.e. since LV networks

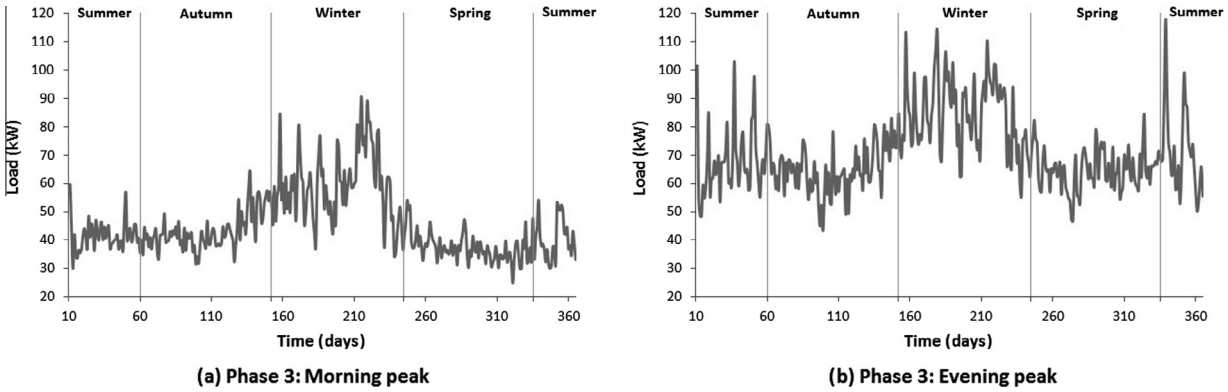

Fig. 2. Daily load characteristics throughout the year.

are more variable than high voltage networks and thus more challenging to precisely forecast).

The scheduling system comprises three main components:

1. The first component is an expert system that forecasts each phase's load profile for the day;
2. The second component is a scheduler that receives the load profile forecast and calculates a charge and discharge schedule;
3. And the third component is the real time operator (RTO): an online system that corrects the schedule dispatch in real time to mitigate forecast errors.

Fig. 3 presents the scheduling system's flow chart. The scheduling system receives load data from the network at the start of each time (t) iteration. An iteration covers a period of 10 min in line with the transformer's frequency of data logging. The load data are corrected by removing the effects of the previous iteration's schedule dispatch and are then filtered to remove fluctuation from the load and yield the underlying moving average. If t is the start of the day, the expert system is called and the scheduler is called. For all other times, the RTO subroutines are called and the schedule is dispatched.

4.2. Battery energy storage system

Fig. 4 contains a simplified schematic of the BES that the scheduling system emulates. The system contains a battery a bank and three programmable inverters on a direct current circuit. Each inverter is connected to an individual phase of the network. This system allows for each inverter to be controlled independently. The individual control of each inverter facilitates the achievement of ancillary scheduling objectives such as load balancing.

The battery bank is defined by a number of variables including the capacity (C), state of charge (SoC), total charge (TC), depth of discharge (DoD), charge rating (CR), discharging rating (DR) and efficiency (BE). C is the maximum amount of energy the battery bank can store. The SoC is the amount of charge or energy stored in the battery bank. TC is an upper limit on the amount of energy stored in the battery bank. DoD is defined as the lower limit on the amount of energy stored in the battery bank. The SoC should not breach the TC and DoD limits to preserve the operational lifespan of the battery bank. DR and CR denote the maximum amount of power that can be discharged to the network or used to charge the battery bank. The inverters have a specified discharge rating (iDR) and charge (iCR) and an efficiency (IE). The variables are set in accordance to the properties of the battery bank and inverters being used or by the user to achieve specific objectives.

The following set of Eqs. (1)–(4) denotes the charging and discharging operations of the BES:

$$SoC_t = SoC_{t-1} + \delta_t \tag{1}$$

where t is the time iteration and δ is the change in charge.

$$\delta_t = \begin{cases} \sum_{i=1}^{3} \delta_{i,t} \times IE \times BE, & if \left(\sum_{i=1}^{3} \delta_{i,t} > 0\right) \bigwedge (SoC_{t-1} < TC) \\ \sum_{i=1}^{3} \delta_{i,t} \times \frac{1}{IE} \times \frac{1}{BE}, & if \left(\sum_{i=1}^{3} \delta_{i,t} < 0\right) \bigwedge (SoC_{t-1} > DoD) \end{cases} \tag{2}$$

where

$$DR \geqslant \delta_t \leqslant CR \tag{3}$$

and

$$iDR \geqslant \delta_{i,t} \leqslant iCR \tag{4}$$

δ_i is the charge provided by inverter i. The BES undergoes charging when the summation of δ_i is positive. The value of the summation is reduced by multiplying it by IE and BE due to the inefficiencies of the inverters and battery bank. There is less power charging the battery bank than what is being drawn from the network. The BES is discharging when the summation of the δ_i is negative. To achieve a specific LV network peak reduction, battery and invertor efficiency factors mean that more power has to be drawn from the battery bank than the value of the peak demand reduction specified. The summation is divided by IE and BE to incorporate this efficiency reduction. The BES can only charge when the SoC is less than TC and can only discharge when SoC is greater than DoD. Unit conversions have been omitted in this paper.

4.3. Expert system to forecast load profiles

The theory behind the expert system developed by Bennett et al. [4] is that certain shapes of load profiles repeat themselves based on external variables such as weather, day of the week, period of the year and corollaries such as total energy use (TEU, the integral of the load profile), MP and EP. A correlation-clustering algorithm was used to identify clusters of load profile patterns. The mean of each cluster was selected to represent the cluster. A discrete classification NN was trained (feed-forward back propagation) with each day's external variables as inputs, and the cluster that the day was a member of was the output. This allows for the selection of a load profile that is most likely to occur. When the expert system is used to forecast, in terms of R^2, it has training accuracies ranging from 0.86 to 0.87 and validation accuracies ranging from 0.81 to 0.84 over the three phases of the network.

The incorporation of the expert system algorithm used in the scheduling system is presented in Fig. 5. The algorithm acquires weather forecasts and uses the information to forecast TEU, MP and EP using time series models. The forecasted information is inputted into the NN and the network gives a score between 0 and 1 for each load profile output neuron. The output neuron with

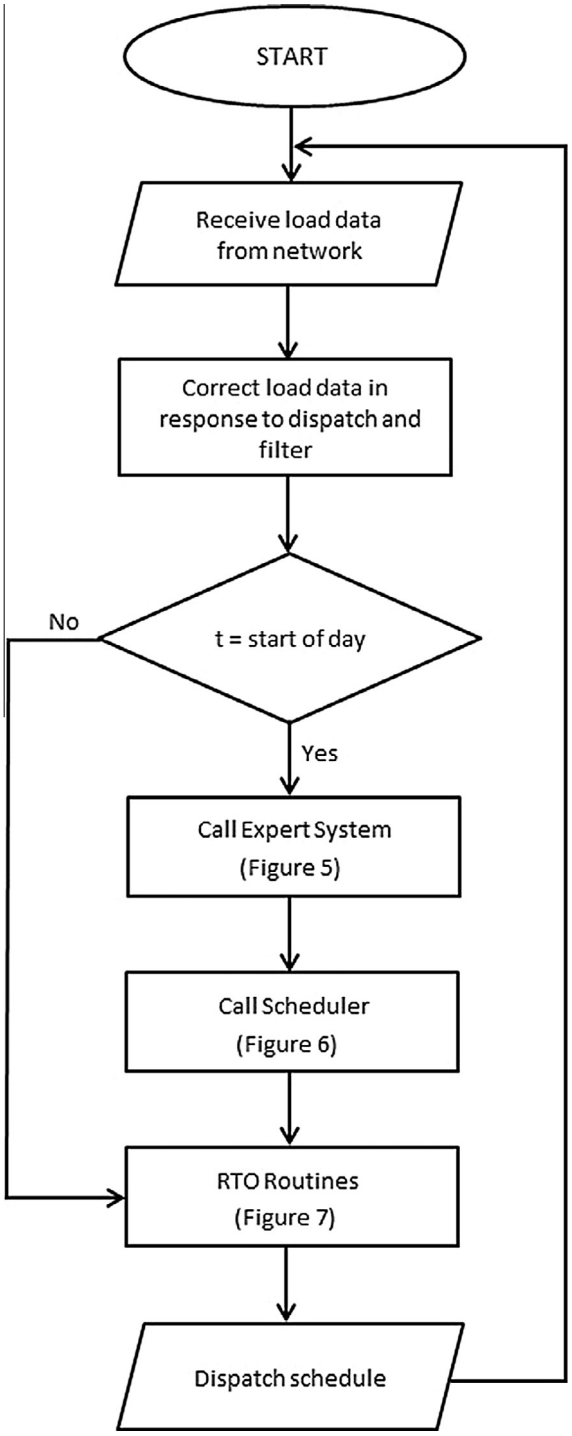

Fig. 3. Scheduling system flow chart.

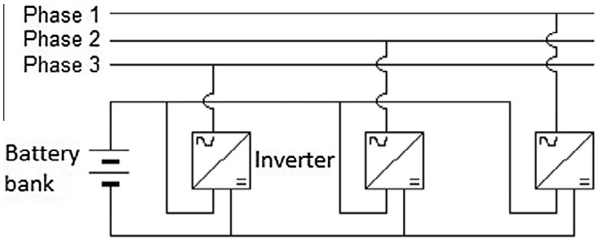

Fig. 4. Simplified battery energy storage system schematic.

the highest score denotes the load profile that is most likely to occur. The selected load profile is adjusted according to the TEU, MP and EP forecast to improve forecast accuracy. The forecasted load profile, defined as *LPf*, is then dispatched to the scheduler. The length of *LPf* is determined by the number of day being forecast. This process is conducted for each phase of the network.

4.4. Scheduler

4.4.1. Overview

The flow chart representing the scheduler is displayed in Fig. 6. The scheduler receives the load forecast from the expert system, identifies significant peaks, initialises the schedule through calculations of *DT* (discharge target), loops through the charging and discharging routines and dispatches the final schedule to the RTO.

The literature displays that the operation of a scheduling system through an objective function optimisation approach attempts to maximise peak demand reduction while minimising the use of BES resources. The optimisation process is constrained by the capacity of the BES and power ratings. If the system were not constrained by the BES capacity, maximum peak demand reduction would equate to the power output rating of the BES. This enables a heuristic to be established through Eqs. 5 and 6:

$$DT_i = \begin{cases} EP_i - iDR, & for\ EP\ period \\ MP_i - iDR, & for\ MP\ period \end{cases} \quad (5)$$

where DT_i is the discharge target for inverter i, which equals the magnitude of the peak minus the discharge rating of the BES. DT_i is a vector where the length of the vector is equal to the length of *LPf*. The DT_i vector is composed of different threshold values that are allotted to the specific MP or EP periods they are calculated from. The scheduler uses the discharge target to create an initial schedule:

$$sched_{i,t} = -(LPf_{i,t} - DT_{i,t}), \quad fort \ni (LPf_{i,t} > DT_{i,t}) \quad (6)$$

where $sched_{i,t}$ is the schedule vector for inverter i at time t and it is calculated for the length of *LPf*. As the scheduler operates, its *SoC* (which is defined as SoC_s) updates according to Eqs. (1)–(4). A negative $sched_{i,t}$ value entails the system will discharge and a positive $sched_{i,t}$ value entails the system will charge. Information that is dispatched to the RTO includes the SoC_s, $sched_{i,t}$ and $DT_{i,t}$.

4.4.2. Identify significant peaks

MP and EP of significance are required to be identified so that schedule initialisation can take place. Peaks are defined according to their amplitude (α) and gradients (m) on either side. The amplitude threshold (t_α) and gradient threshold (t_m) are determined by historical data or arbitrarily by the user. Significant peaks are identified according to the following algorithm:

1. *LPf* is subdivided into corresponding days.
2. The *LPf* for each day is split into morning and evening periods (MP and EP periods).
3. α equals the greatest value of the period and the corresponding element is recorded.
4. If $\alpha \geqslant t_\alpha$ and $abs(m) \geqslant t_m$, then the peak is considered to be significant.

Schedule initialisation is conducted according to Eqs. 5 and 6.

4.4.3. Battery charging routines

The *SoC* is imported from the RTO in order to set the initial *SoC* for the schedule. The initial battery charging routine charges the battery bank according to Eq. 7:

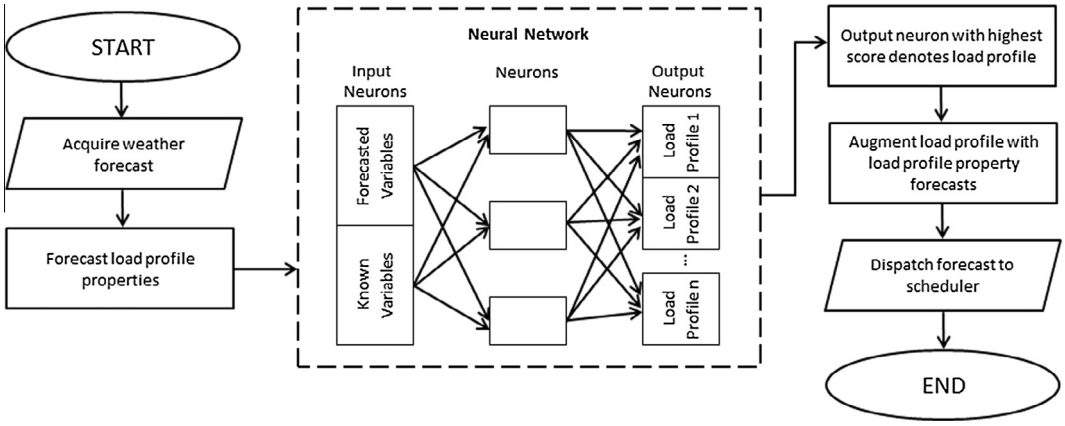

Fig. 5. Expert system.

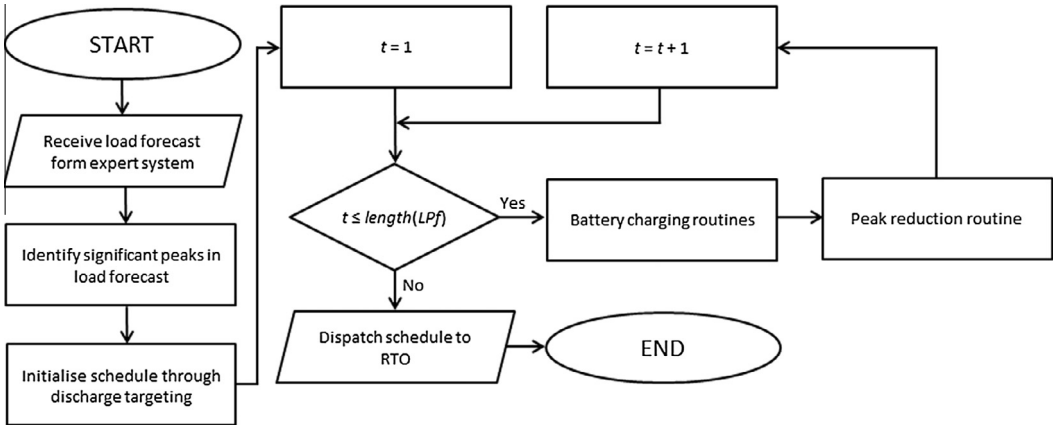

Fig. 6. Scheduler.

$$sched_{i,t} = \begin{cases} iCR, \ if\,(SoC_{s,t} < (TC - 3 \times iCR)) \bigwedge (LPf_{i,t} < DT_{i,t}) \\ (TC - SoC_{s,t}) \div 3, \ if\,(SoC_{s,t} < TC) \bigwedge (LPf_{i,t} < DT_{i,t}) \end{cases} \quad (7)$$

The equation states that while the SoC_s is less than TC, the battery bank will charge at the rate iCR. When the SoC_s nears TC (i.e. $TC - 3 \times iCR$) the remaining charge is divided across the three phases so that SoC_s does not exceed TC.

A valley fill charging routine commences if SoC_s equals TC before $LPf_{i,t} \geqslant DT_{i,t}$. The purpose of the valley fill charging routine is to schedule charging specifically during low load periods and to balance phases by charging more from the least loaded phases. The valley filling routine operates by establishing a target vector CT as the minimum LPf_i value over the charging period and iteratively increasing the value of CT until the area between LPf_i and CT equals the amount of energy that is required to charge the battery bank. The charging period is defined between a start element (se) and a finish element (fe), which are calculated using Eqs. (8)–(10):

$$se = \min(t), \quad for\ t \ni (LPf_{i,t} < DT_{i,t}) \bigwedge (1 \leqslant i \leqslant 3) \quad (8)$$

$$fe = \max(t), \quad for\ t \ni (LPf_{i,t} < DT_{i,t}) \bigwedge (1 \leqslant i \leqslant 3) \quad (9)$$

where

$$(1 \bigvee pp) > t < (np \bigvee length\ (LPf)) \quad (10)$$

The calculation of se and fe is constrained either by the start of the scheduling period or the previous peak period (pp) and the next peak period (np) or by the end of the scheduling period with respect to the current t. This allows CT to be calculated by Eq. (11). The iterative increase commences by adding an '*adjust*' constant adj as represented by Eq. (12). The iterative process ceases when SoC_s at the end of the charge period equals TC.

$$CT_{l-1} = \min(LPf_{i,t}), \quad for\ (se \leqslant t \leqslant fe) \bigwedge (1 \leqslant i \leqslant 3) \quad (11)$$

$$CT_l = CT_{l-1} + adj, \quad while\ SoC_{s,fe} < TC \quad (12)$$

where l is the iteration number. While the iterative process continues, the schedules for each phase are calculated:

$$sched_{i,se \to fe} = \begin{cases} CT_l - LPf_{i,se \to fe}, \ if\,(CT_l - LPf_{i,se \to fe}) \leqslant iCR \\ iCR, \ if\,(CT_l - LPf_{i,se \to fe}) > iCR \end{cases} \quad (13)$$

The valley fill charging routine enables the scheduling system to charge the BES more from the phase that is expected to have the least load and less from the phase expected to have the highest load.

Fig. 7 graphically depicts the valley fill charge routine over a particular phase's LPf. The shaded areas denote the operations of the BES system. The charge period starts at se and finished at fe (Eqs. 8 and 9). It is assumed that the LPf for the other two phases are greater in magnitude during the charge period. The initial CT is the minimum value of the LPf of the three phases (Eq. (11)) which was calculated to be 23 kW. The CT increased from 23 kW in a loop (Eq. (12)) by adj each iteration until the amount of energy that is required to charge the battery bank from $SoC_{s,t}$ to TC was available. The final CT was calculated to be 45 kW. The area

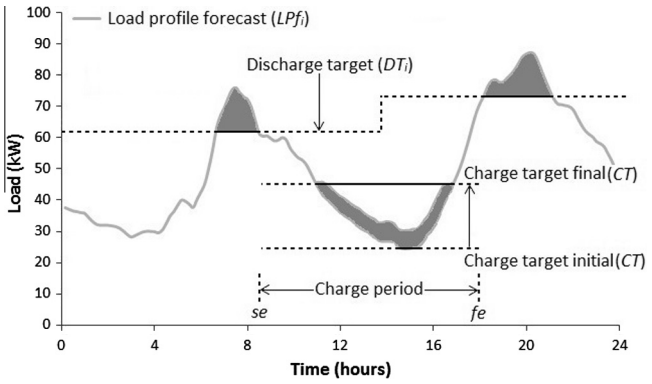

Fig. 7. Valley fill charge routine.

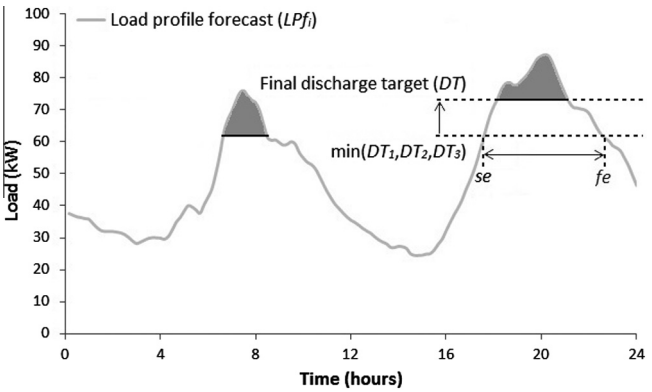

Fig. 8. Peak reduction routine.

between the *LPf* and the final *CT* is not completely allocated to charging due to the rate of charging is constrained by *CR* and *iCR*. The difference between *CT* and the other phases' *LPf* is less than the phase presented, therefore less energy is used to charge the battery bank from the other two phases.

4.4.4. Peak reduction routine

When t is such that $LPf_{i,t} > DT_{i,t}$, the peak reduction routine commences. This routine constrains the initial peak discharge schedule according to the available BES resources. The first step involves identifying how much energy is available for discharging:

$$e_a = \begin{cases} SoC_{s,t-1} - DoD, & if\ SoC_{s,t-1} > DoD \\ 0, & if\ SoC_{s,t-1} \leqslant DoD \end{cases} \quad (14)$$

where e_a is the available energy. The next step is to identify start and finish elements (i.e. *se* and *fe*) of the peak discharge schedule. *se* equals t when t is such that $LPf_{i,t} > DT_{i,t}$. *fe* is calculated by Eqs. 15 and 16:

$$fe = \max(t),\ for\ t \ni (LPf_{i,t} > DT_{i,t}) \bigwedge (1 \leqslant i \leqslant 3) \quad (15)$$

where

$$se > t \leqslant edp \quad (16)$$

where *edp* is the end of the discharge period. Identifying the peak discharge period allows for the calculation of how much energy is required to achieve the initial schedule:

$$e_r = \sum_{t=se}^{fe} \sum_{i=1}^{3} sched_{i,t} \quad (17)$$

where e_r is the energy required. If $e_a \geqslant e_r$ no further actions are required, else an iterative $DT_{i,se\to fe}$ adjustment process as described in Eqs. (18) and (19) should be applied to increase $DT_{i,t}$:

$$DT_{i,se\to fe,l-1} = \min\left(DT_{i,se\to fe}\right), \quad for\ 1 \leqslant i \leqslant 3 \quad (18)$$

$$DT_{i,se\to fe,l} = DT_{i,se\to fe,l-1} + adj, \quad while\ e_r > e_a \quad (19)$$

$sched_{i,t}$ is updated according to Eq. (20) and then e_r is updated according to Eq. (17).

$$sched_{i,se\to fe} = \begin{cases} -\left(LPf_{i,se\to fe} - DT_{i,se\to fe,l}\right), & if\ \left(LPf_{i,se\to fe} - DT_{i,se\to fe,l}\right) > 0 \\ 0, & if\ \left(LPf_{i,se\to fe} - DT_{i,se\to fe,l}\right) < 0 \end{cases} \quad (20)$$

Similar to the valley fill charging routine, by increasing $DT_{i,t}$ the peak reduction routine also achieves load balancing by discharging more energy to the phase with the highest load and less to the phase with the least load.

Fig. 8 depicts the peak reduction routine for an EP period over a particular phase's *LPf*. It is assumed that the *LPf* for the other two phases are less than the presented *LPf*. In this circumstance there is an insufficient SoC_s for the peak to be reduced according to the initial schedule. The discharge period starts at *se* and finished at *fe*. The routine sets each DT_i to the minimum of the set (Eq. (18)). The DT_i for each phase increases in a loop (Eq. (19)) until the amount of energy required to reduce the peak to DT_i (Eq. (17)) equal the energy available in the battery bank (Eq. (14)). The difference between DT_i and the peaks of the other two phases are less than the presented phase. In turn, the energy allocated to reduce the peaks of the other two phases is less than the presented.

4.5. Real time operator

4.5.1. Overview

There are two types of scheduling system failure that are resultant from the inherent error associated with forecasting volatile LV networks. The first type relates to calculated schedules not aligning well with the load experienced in the network. The second type stems from the BES resources being prematurely depleted during the peak period, resulting in a sudden load spike. The primary function of the RTO is to analyse the network's load in real time, compare it against the expert system forecast and engage in remedial measures to prevent these two failure types from occurring. The secondary function is to load balance the network under battery bank charging. The RTO has no prior knowledge of the future other than what forecasts provide.

The RTO first receives historical load (L), SoC_s, $sched_{i,t}$ and $DT_{i,t}$ information from previous stages in the scheduling system. In accordance with Fig. 9, the RTO engages in *DT* adjustment, forecasts load for the current time interval, creates charging and discharging routines and dispatches the current time intervals schedule to the inverters and battery bank.

4.5.2. Discharge target adjustment

The scheduling system has a reliance on the establishment of *DT* to emulate the optimal scheduling of the BES system. The increase or decrease of $DT_{i,t}$ directly controls how much the BES system discharges into the network. As $DT_{i,t}$ increases, the amount of discharge decreases. Conversely, as $DT_{i,t}$ increases, the amount of discharge decreases. Through adjustments of $DT_{i,t}$ and then $sched_{i,t}$, the resource depletion failure state can be avoided.

Information to base the adjustments is generated from the comparison between the rate of energy use anticipated by the scheduler recorded in SoC_s and the real rate of energy use recorded in *SoC*. Fig. 10 highlights information derived from the SoC_s and *SoC* vectors. The local gradients for SoC_s and *SoC* are calculated and

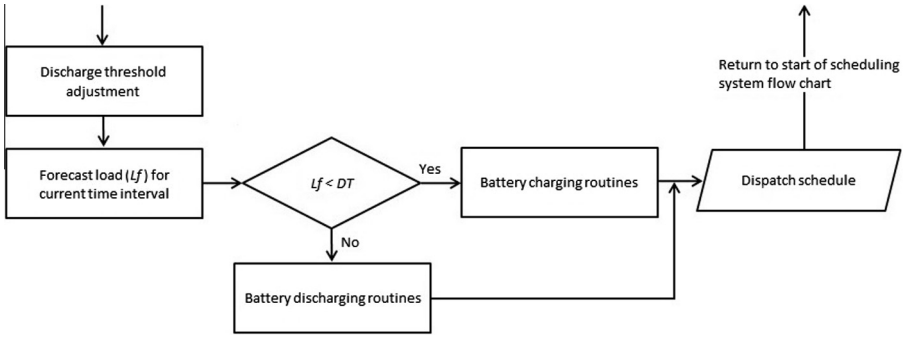

Fig. 9. Real time operator.

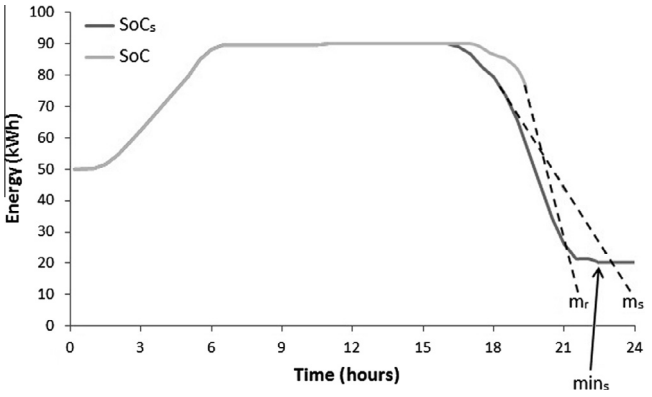

Fig. 10. Local rates of energy use.

defined as m_s and m_r respectively. If $abs(m_r) > abs(m_s)$ then the rate of energy use is not in accordance with the scheduler's estimation. If the rate of energy use continues at m_r there could potentially be a failure. The point when the scheduler estimates that the discharging period is over is defined as min_s.

The point when *SoC* will equal *DoD* at current m_r is calculated by Eq. (21):

$$min_r = \frac{SoC_{s,t-1} - DoD}{abs(m_r)} \tag{21}$$

Increases to $DT_{i,t}$ are calculated according to Eqs. (22)–(25):

$$a_1 = \begin{cases} \frac{abs(m_r)-abs(m_s)}{y-t+1}, & if\ abs(m_r) > abs(m_s) \\ 0, & if\ abs(m_r) \leqslant abs(m_s) \end{cases} \tag{22}$$

$$a_2 = \begin{cases} \frac{SoC_{s,t-1}-SoC_{t-1}}{y-t+1} \times \left(1 - \frac{SoC_{t-1}-DoD}{TC}\right), & if\ SoC_{t-1} < SoC_{s,t-1} \\ 0, & if\ SoC_{t-1} \geqslant SoC_{s,t-1} \end{cases} \tag{23}$$

$$DT_{i,t\to y} = a_1 + a_2 \tag{24}$$

where

$$y = \begin{cases} \omega, & if\ EP \\ \frac{\omega}{2}, & if\ MP \end{cases} \tag{25}$$

where a_1 is the increase due to the real rate of energy use being greater than the estimated, a_2 is the increase due to there being less energy available at time t than what was estimated, y is the specific EP or MP time period and ω is the number of time intervals in a day. In this case there are 144 10-min intervals in a day. $DT_{i,t}$ is adjusted from time t to the end of the period *fe*.

Since load in the LV distribution network is highly variable, decreases to $DT_{i,t}$ may be required to maximise peak reduction. Decreases to $DT_{i,t}$ are conducted according to Eqs. (26)–(28):

$$b_1 = \begin{cases} \frac{abs(m_r)-abs(m_s)}{y-t+1}, & if (abs(m_r) < abs(m_s)) \bigwedge (min_r > min_s) \\ 0 & , if\ abs(m_r) \geqslant abs(m_s) \end{cases} \tag{26}$$

$$b_2 = \begin{cases} \frac{SoC_{s,t-1}-SoC_{t-1}}{y-t+1} \times \left(\frac{SoC_{s,t-1}-DoD}{TC}\right), & if\ (SoC_{t-1} > SoC_{s,t-1}) \bigwedge (min_r > min_s) \\ 0, & if\ SoC_{t-1} \leqslant SoC_{s,t-1} \end{cases} \tag{27}$$

$$DT_{i,t\to y} = b_1 + b_2 \tag{28}$$

where b_1 is the decrease due to the real rate of energy use being less than the estimated, b_2 is the decrease due to there being more energy available at time t and y is calculated by Eq. (25). Both b_1 and b_2 are negative values or equal to zero. The recalculation of $sched_{i,t}$ in response to $DT_{i,t}$ adjustment is conducted using Eq. (35).

4.5.3. Load forecast

The load on each phase is forecasted for the current time interval. This enables the best schedule for the current time interval to be calculated. Each phase has its own forecast model. The coefficients of the models are calculated using historical load data of the particular phase and regression. The general forecast model is described by Eq. (29):

$$Lf_t = \beta_1 L_{t-1} + \beta_2 L_{t-2} + \beta_3 L_{t-day} + \beta_4 L_{t-7\times day} + \beta_5 L_{t-14\times day} + \varepsilon \tag{29}$$

where Lf_t is the load forecast for time t, L is the historical load, β terms are model coefficients and ε is the model's error term. Half of the historical load dataset was used for coefficient estimation and the other half was used for validation. Each phase's validation R^2 equalled 0.99 and mean absolute percentage error equalled one per cent. The models had slight positive autocorrelation in the error terms entailing that if iterative forecasts were made, forecasts further from t will significantly deviate from the load that will occur.

4.5.4. Battery charging and discharging routines

To ensure that load balancing is maintained, the Lf_t for the current time interval t is used to evaluate the magnitude of the loads across the phases and a single time interval version to the scheduler's valley fill charging routine is engaged. The initial schedule $sched_{i,t}$ provided by the scheduler dictates the amount of energy that is required to charge the battery bank at the current t for each i. Thus the first step in the process is calculating the required energy which is the aggregate of $sched_{i,t}$ for the current t:

$$e_r = \sum_{i=1}^{3} sched_{i,t} \tag{30}$$

The minimum value of the three load forecasts is set as the initial *CT*. Through an iterative process (Eqs. (31)–(34)), *CT* is increased according to an *adj* constant, and $sched_{i,t}$ and e_a are calculated according to the new *CT*:

$$CT_l = \min\ (Lf_{1-3,t}) \tag{31}$$

$$CT_l = CT_{l-1} + adj, \quad while\ e_a < e_r \tag{32}$$

$$sched_{i,t} = \begin{cases} CT_l - Lf_{i,t}, & if\ ((CT_l - Lf_{i,t}) \leqslant iCR) \bigwedge ((CT_l - Lf_{i,t}) \geqslant 0) \\ iCR, & if\ (CT_l - Lf_{i,t}) > iCR \\ 0, & if\ (CT_l - Lf_{i,t}) < 0 \end{cases} \tag{33}$$

and

$$e_a = \sum_{i=1}^{3} sched_{i,t} \tag{34}$$

The discharge schedule is updated in real time to mitigate misalignments between the LPf_i and actual load in the network and is must be updated in response to $DT_{i,t}$ adjustments. The battery discharging routine commences for the current *t* when $Lf_{i,t} > DT_{i,t}$ and calculates a new $sched_{i,t}$ using a single time interval version of Eq. (6). The new discharge schedule is calculated in Eq. (35):

$$sched_{i,t} = \begin{cases} -(Lf_{i,t} - Dt_{i,t}), & if\ (Lf_{i,t} - Dt_{i,t}) \leqslant iDr \\ -iDR, & if\ (Lf_{i,t} - Dt_{i,t}) > iDr \end{cases} \tag{35}$$

5. Results

5.1. Scheduler

A BES system with a *C* of 100 kilowatt hours (kW h), *TC* of 90 per cent (90 kW h), *DoD* of 20 per cent (20kW h), *DR* of 40 kilowatt (kW), *CR* of 15 kW, *iDR* of 15 kW, *iCR* of 6 kW, *BE* of 97 per cent and *IE* of 97 per cent was applied in the SEQ LV network previously described. An initial SoC_s was selected to be 50kW h. The expert system provided three days (72 h) of consecutive *LPf* for each phase. As previously noted, the training accuracy of the expert system is terms of R^2 ranged from 0.86 to 0.87 and the validation accuracy ranged from 0.81 to 0.84.

Fig. 11 contains the results of the scheduler for each phase and the estimated SoC_s for the duration of the three-day forecast period. The $sched_i$ for each phase is displayed through the results of simulating the dispatch of the schedule for the BES system. When the system is charging, the schedule dispatch is greater than the forecast. When the system is discharging over the peak period, the schedule dispatch is less than the forecast. The magnitude of the load during the peak period of the forecast with the dispatched schedule applied is indicative of the *DT* for the period. Charging specifically occurs in the valleys and discharging specifically occurs during the peak period. The SoC_s is maintained between the *DoD* and *TC* throughout the period. The SoC_s decreases as the system is discharging and increases as the system is charging.

For the first period when charging commences, it can be seen that the scheduler sets the BES system to charge more from the phase that is estimated to have the least load (phase 3) and least from the phase estimated to have to the highest load (phase 1). Similar to the first charge period, the first discharge period indicates that more energy is allocated to the phase that is anticipated to have the highest load (phase 1) and least amount of energy is allocated to the phase that is anticipated to have the least load (phase 2). These results display that the scheduler attempts to achieve the secondary objective of load balancing.

5.2. Real time operation

Using the same BES system properties and initial *SoC* of 20 kW h, Fig. 12 illustrates the difference between the dispatch of the schedule with and without the utilisation of the RTO adjustments. Fig. 12a highlights the BES resource depletion failure state. Without the RTO, the BES did not have enough capacity to continuously discharge throughout the entire peak period leading to a sharp increase in load on the network measured at the LV transformer. Fig. 12b illustrates how the RTO module of the scheduling system overcomes the limitations of the scheduling forecasts. At the 20th hour mark, the RTO anticipates that there will not be a sufficient amount of energy available if it continues to follow the initial dispatch schedule. As a result, it increases the *DT* and the schedule is recalculated. At the 21st hour mark, the RTO temporarily decreases *DT*.

To simulate the scheduling software analogous to real world conditions, the software was provided with unfiltered load data and imperfect forecasts. The results of the simulation for a 72-h period are displayed in Fig. 13. This figure shows a comparison between the original load and the results of the scheduling system dispatching charging and discharging schedules to the BES system for each phase. The *SoC* was recorded through the period and did not breach the *TC* and *DoD* limits. In comparison to the *LPf*, the load observed in the network exhibits a greater degree of variability as seen by the occurrence of double peaks within a peak demand period. From the results, the scheduling system was able to reduce peak demand across each phase and charge the battery bank during valleys. The scheduling system achieved its secondary objective of load balancing. For the second day of the simulation period, more energy was allocated to phases 1 and 2, which had higher loads than phase 3. During the demand valleys, phases with lower loads were charged more than phases with higher loads.

5.3. Battery energy storage capacity sizing

The developed scheduler module of the scheduling system also provides the architecture for a tool that can be used for optimally sizing BES in LV networks. This can be achieved by inputting a particular LV networks historical load data into the scheduling system as well as the simulated BES specifications (i.e. *C*, *TC*, *DoD*, *CR*, *DR*, etc.). The user can consider a range of commercially available BES and their particular specifications or alternatively use an optimisation routine (e.g. particle swarm, gradient-decent, Lagrangian, etc.) to identify a BES system to achieve specific valley fill and peak reduction objectives. The estimated goal performance (e.g. peak demand reduction, power quality improvement, load balancing, better solar PV utilisation, etc.) for a simulated BES system can then also be used as empirical evidence for undertaking cost-benefit assessments. Such empirical evidence is important for electricity distribution utilities seeking to formulate sound business cases for installing BES in LV networks.

An example of the use of the scheduler for BES sizing is displayed in Fig. 14. This example uses the same system parameters as the system used to demonstrate the results of the scheduler. *C* is altered to find the optimal size to achieve maximum peak reduction given the other system parameters and each simulation is run for a period of 200 days. The results for each phase of the simulations are presented in terms of mean daily peak reduction and the mean amount of energy allocated to reduce the peak.

When the capacity of the BES system is relatively low, the scheduler is less able to reduce the peaks. Phases 1 and 3 had the greater peak reductions than phase 2 by 6–7 kW. As a corollary, phases 1 and 3 were allocated a greater amount of energy to reduce the peaks. The reason for this is that phases 1 and 3 experiences higher loads than phase 2. The scheduler is better able to

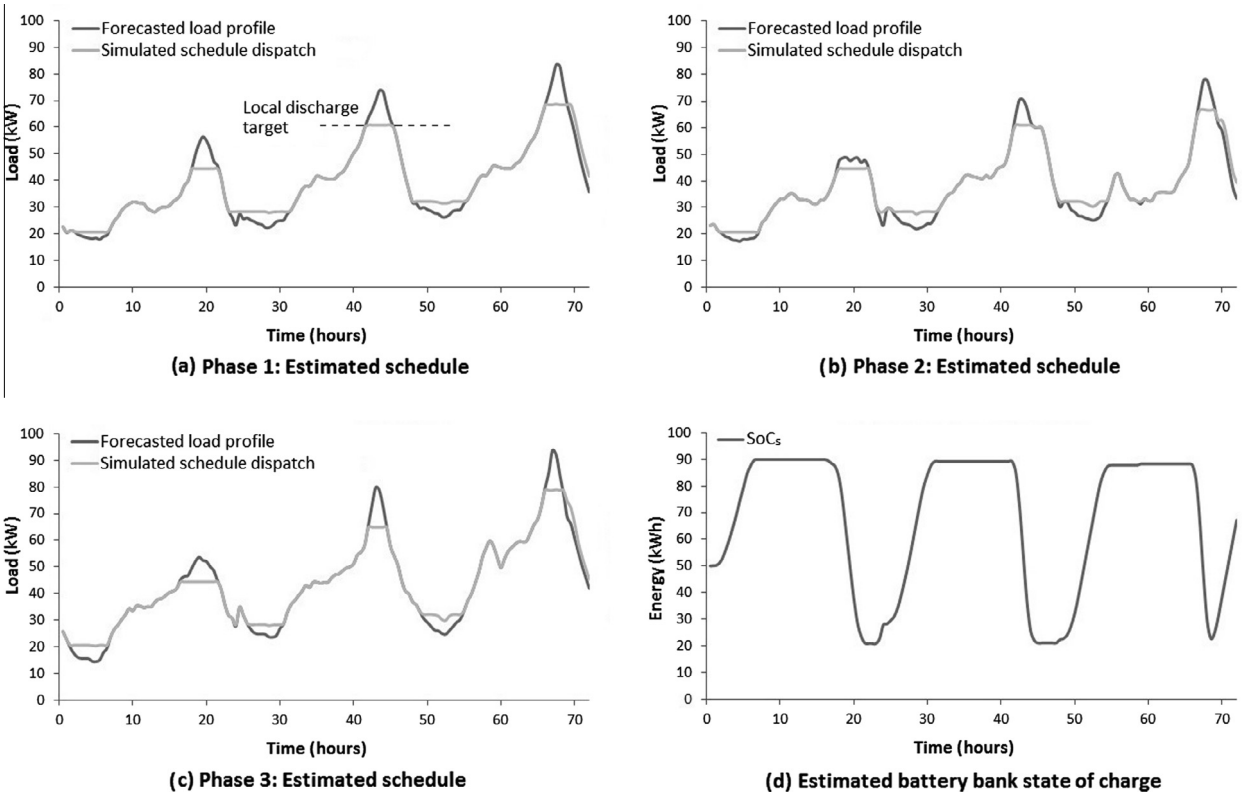

Fig. 11. Scheduler results.

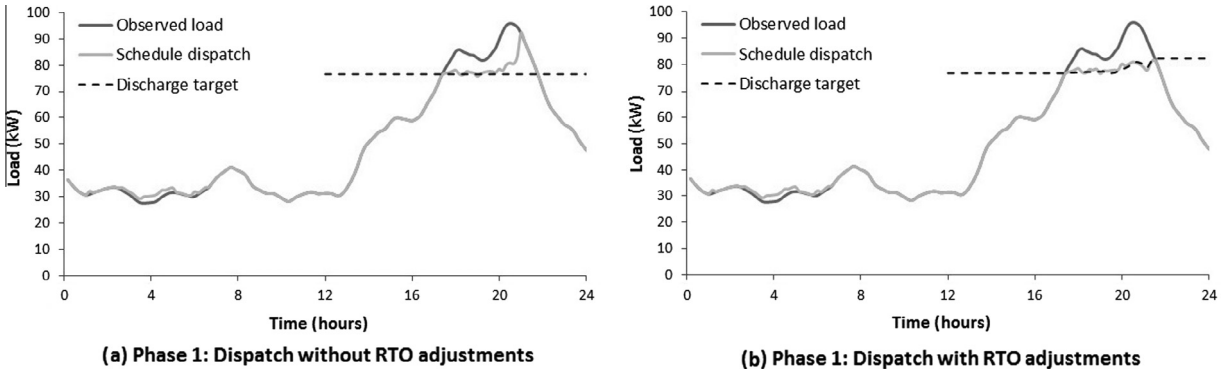

Fig. 12. Discharge target augmentation process.

reduce the peaks as the capacity of the BES system increases. Phase 2 has the highest incremental gain in peak reduction. The incremental gains for phases 1 and 3 are curtailed after the BES system capacity reaches 100kW h. After 100kW h, the incremental gains continue for phase 2 until 175kW h. At this point, additional investment in BES system capacity would not have a substantial effect on peak reduction. While a full life cycle cost-benefit assessment (outside scope of current paper) would precisely define the optimal BES sizing for this particular SEQ LV network examined, Fig. 14 indicates that a 100kW h capacity would likely be optimal.

6. Conclusion and future work

This research proposed a forecast and heuristic based three-phase BES scheduling system for the LV distribution network. The primary goal of the scheduling system was to charge the BES during periods of low demand and discharge during periods of high demand: peak shaving and valley filling. The secondary objective was to balance the load across the three phases. The scheduling system is composed of three main components: an expert system, a scheduler and a RTO. The expert system is used to produce load profile forecasts. The scheduler receives the load profile forecast and creates an initial schedule. The RTO, which analyses recent historical load data against the scheduler's output, engages in remedial measures if required. The RTO is primarily required to mitigate errors caused by the imperfect forecasted load profiles.

When implementing a BES system with particular specifications in the case study SEQ LV network, the developed scheduler was able to take the forecasted load profiles and produce a charging and discharging schedule. It was observed that the scheduler was able to set the schedule to charge during periods of low demand and discharge period peak demand periods while achieving its

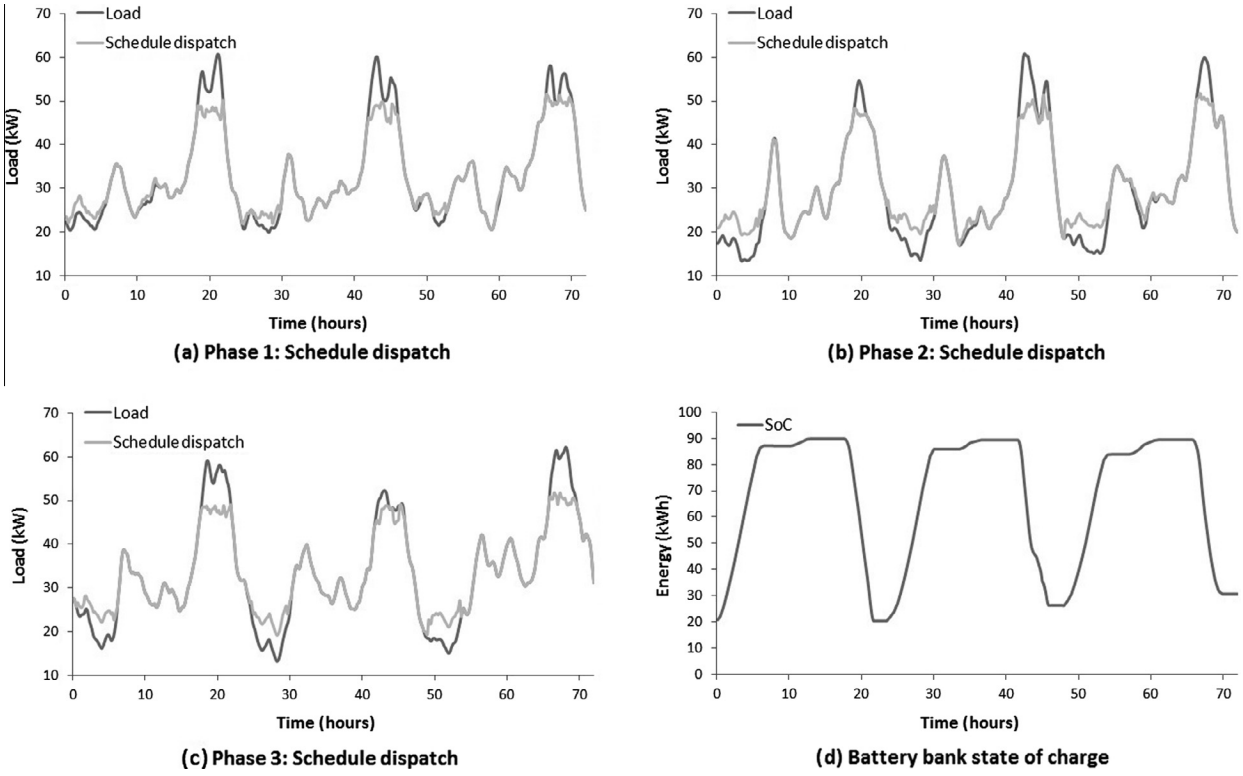

Fig. 13. Real time operator results.

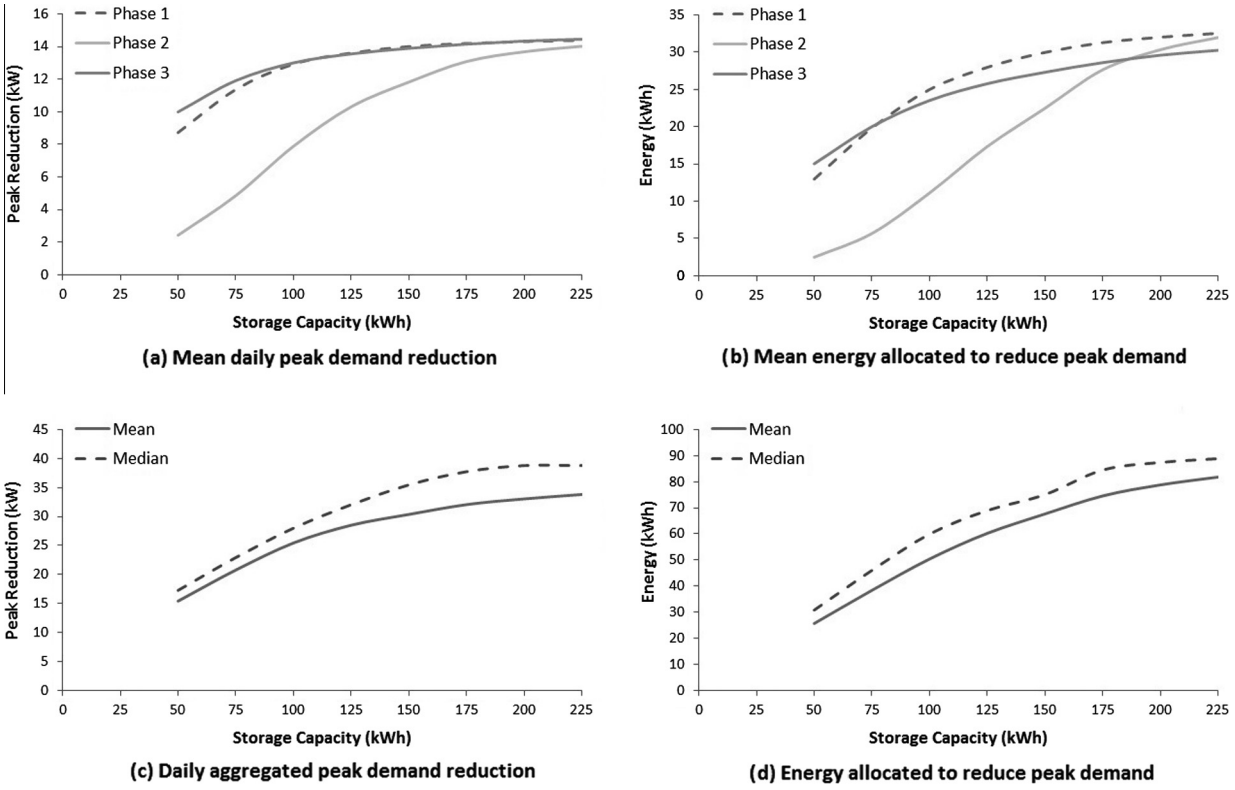

Fig. 14. Sizing battery energy storage system.

secondary objectives of balancing the load. Results display that more energy was charged from the phase with the least load and discharged to the phase with the highest load.

To achieve the primary and secondary goals in real time, for each time interval the RTO adjusts the schedule to mitigate initial scheduling error. The RTO does this by increasing or decreasing the

amount of energy that is discharged based on discrepancies between the estimated SoC_s and the actual SoC. When the real rate of energy use is greater than the rate estimated by the scheduler, the RTO decreases rate of discharge. The RTO may correct the adjustment if the real rate of energy usage becomes less than the estimated rate. The RTO ensures load balancing during charging periods by redistributing the amount of energy that the battery bank is scheduled to be charged by to the least loaded phases. The results from operating the scheduling system in real time displayed, like the scheduler, the system was able to reduce peak demand, charge during low demand periods and balance phases. More energy was allocated to reduce the peaks of high loaded phases and the least loaded phases were charged from more.

The scheduler component was able to be repurposed and used to size BES systems in a particular LV network to achieve a set of desired goals (e.g. certain peak demand reduction) or gauge a particular system's performance. To demonstrate this, simulations were run using the scheduler's routines with different battery bank capacities. The peak demand reduction performance increased as the capacity of the battery bank increased. Performance gains started to decreased after 100kW h and were hampered after 175kW h. This indicated for the specific BES system, the capacity that was most likely to be optimal was 100kW h.

In summary, the scheduling system was able to achieve its desired purpose and there are avenues for the development of BES system sizing applications. Future work on this research and development project involves three main stages. The first stage is to further improve the LV distribution network forecast accuracy. The second stage involves coding and installing scheduling firmware into an innovative three-phase LV network STATCOM (static synchronous compensator) with integrated BES that has recently been developed by one of the industry partners. The third stage is to implement and test the intelligent STATCOM with integrated BES in a trial LV network located in SEQ, Australia.

Acknowledgements

This research has been facilitated by funding provided by the Queensland State Government 2012–2014 Partnership Grant. The grant has allowed Griffith University, Elevare, Ergon Energy and Energex to conduct collaborative applied research on smart-grid theory, technology and applications such as STATCOMs, energy storage systems and integrated solar PV. The goal is to have smart-grid technology in place that will reduce peak demand and consumption of energy from traditional and renewable sources, actively manage power quality and create value for network operators and customers. The authors are grateful to Energex for providing the data that made this research possible.

References

[1] Australian Energy Regulator. State of the energy market 2013 [Internet]. Australian Energy Regulator; 2013. <www.aer.gov.au/node/23147> [cited 2014 August 5].
[2] Energex. Annual performance report 2012/13 [Internet]. Energex; 2013. <www.energex.com.au/__data/assets/pdf_file/0003/167322/Annual-Report-2012-13.pdf> [cited 2014 Aug 4].
[3] Australian Energy Market Operator. National electricity forecast report: for the national electricity market [Internet]. Australian Energy Market Operator; 2014. <www.aemo.com.au/Electricity/Planning/Forecasting/National-Electricity-Forecasting-Report> [cited 2014 Aug 5].
[4] Bennett CJ, Stewart RA, Lu JW. Forecasting low voltage distribution network demand profiles using a pattern recognition based expert system. Energy 2014;67:200–12.
[5] Alam MJE, Muttaqi KM, Sutanto D. Mitigation of rooftop solar PV impacts and evening peak support by managing available capacity of distributed energy storage systems. IEEE Trans Power Syst 2013;28(4):3874–84.
[6] Ausgrid. Effect of small solar photovoltaic (PV) systems on network peak demand [Internet]. Ausgird; 2011. <www.ausgrid.com.au/Common/Aboutus/Newsroom/Discussions/~/media/Files/About%20Us/Newsroom/Discussions/Solar%20PV%20Research%20Paper.ashx> [cited 2014 Aug 6].
[7] Dunn B, Kamath H, Tarascon J. Electrical energy storage for the grid: a battery of choices. Science 2011;334(6058):928–35.
[8] Higgins A, Grozev G, Ren Z, Garner S, Walden G, Taylor M. Modelling future uptake of distributed energy resources under alternative tariff structures. Energy 2014. http://dx.doi.org/10.1016/j.energy.2014.07.010. July 28.
[9] Weiss M, Patel M, Junginger M, Perujo A, Bonnel P, Grootveld G. On the electrification of road transport – learning rates and price forecasts for hybrid-electric and battery-electric vehicles. Energy Policy 2012;48:374–93.
[10] Jayasekara N, Wolfs P, Masoum MAS. An optimal management strategy for distributed storages in distribution networks with high penetrations of PV. Electric Power Syst Res 2014;116:147–57.
[11] Marwali MKC, Haili M, Shahidehpour SM, Abdul-Rahman KH. Short term generation scheduling in photovoltaic-utility grid with battery storage. IEEE Trans Power Syst 1998;13(3):1057–62.
[12] Lu B, Shahidehpour M. Short-term scheduling of battery in a grid-connected PV/battery system. IEEE Trans Power Syst 2005;20(2):1053–61.
[13] Lee TY. Operating schedule of battery energy storage system is a time-of-use rate industrial user with wind turbine generators: a multipass iteration particle swarm optimization approach. IEEE Trans Energy Convers 2007;22(3):774–82.
[14] Oudalov A, Cherkaoui R, Beguin A. Sizing and optimal operation of battery energy storage system for park shaving application. Power Tech; 2007 July; Lausanne, Switzerland. IEEE; 2007. p. 1–5.
[15] Xu Y, Xie L, Singh C. Optimal scheduling and operation of load aggregator with electric energy storage in power markets. North American Power Symposium; 2010 September; Arlington, TX, USA. IEEE; 2010. p. 1–7.
[16] Hu W, Chen Z, Bak-Jensen B. Optimal operation strategy of battery energy storage system to real-time electricity price in Denmark. Power and Energy Society General Meeting; 2010 July; Minneapolis, MN, USA. IEEE; 2010. p. 1–7.
[17] Koutsopoulos I, Hatzi V, Tassiulas L. Optimal energy storage control policies for the smart power grid. Smart Grid Communications; 2011 October; Brussels, Belgium. IEEE; 2011. p. 475–80.
[18] Grillo S, Marinelli M, Massucco S, Silvestro F. Optimal management strategy of a battery-based storage system to improve renewable energy integration in distribution networks. IEEE Trans Smart Grid 2012;3(2):950–8.
[19] Matallanas E, Castillo-Cagigal M, Gutierrez A, Monasterio-Huelin F, Caanamo-Martin E, Masa D, et al. Neural network controller for active demand-side management with PV energy in the residential section. Appl Energy 2012;91:90–7.
[20] Castillo-Cagigal M, Caanamo-Martin E, Matallanas E, Masa-Bote D, Gutierrez A, Monasterio-Huelin F, et al. PV self-consumption optimization with storage and active DSM for the residential sector. Solar Energy 2011;85:2338–48.
[21] Rowe M, Yunusov T, Haben S, Singleton C, Holderbaum W, Potter B. A peak reduction scheduling algorithm for storage devices on the low voltage network. IEEE Trans Smart Grid 2014;5(4):2115–24.
[22] Rowe M, Yunusov T, Haben S, Holderbaum W, Potter B. The real-time optimisation of DNO owned storage devices on the LV network for peak reduction. Energies 2014;7:3537–60.
[23] Arghandeh R, Woyak J, Onen A, Jung H, Broadwater RP. Economic optimal operation of community energy storage systems in competitive energy markets. Appl Energy 2014;135:71–80.
[24] Sanseverino ER, Silvestre ML, Zizzo G, Gallea R, Quang NN. A self-adapting approach for forecast-less scheduling of electrical energy storage systems in a liberalized energy market. Energies 2013;6(11):5738–59.
[25] Riffonneau Y, Bacha S, Barruel F, Ploix S. Optimal power flow management for grid connected PV system with batteries. IEEE Trans Sustainable Energy 2011;2(3):309–20.
[26] Haben S, Ward J, Greetham DV, Singleton C, Grindrod P. A new error measure for forecasts of household-level, high resolution electrical energy consumption. Int J Forecasting 2014;30:246–56.
[27] Kabir MN, Mishra Y, Ledwich G, Xu Z, Bansal RC. Improving voltage profile of residential distribution systems using rooftop PV and battery energy storage systems. Appl Energy 2014;134:290–300.
[28] Bennett CJ, Stewart RA, Lu JW. Autoregressive with exogenous variables and neural network short-term load forecast models for residential low voltage distribution networks. Energies 2014;7(5):2938–60.